SLAC-TN--91-3

DE92 002223

NEUTRON DOSIMETRY AT SLAC: NEUTRON SOURCES AND INSTRUMENTATION*

J. C. Liu, T. M. Jenkins, R. C. McCall, and N. E. Ipe

Stanford Linear Accelerator Center,
Stanford University, Stanford, CA 94309

ABSTRACT

This report summarizes in detail the dosimetric characteristics of the five radioisotopic type neutron sources (^{238}PuBe, ^{252}Cf, ^{238}PuB, $^{238}PuF_4$, and ^{238}PuLi) and the neutron instrumentation (moderated BF_3 detector, Anderson-Braun (AB) detector, AB remmeter, Victoreen 488 Neutron Survey Meter, Beam Shut-Off Ionization Chamber, ^{12}C plastic scintillator detector, moderated indium foil detector, and moderated and bare TLDs) that are commonly used for neutron dosimetry at the Stanford Linear Accelerator Center (SLAC).

MASTER

* Work supported by Department of Energy contract DE-AC03-76SF00515.

DISTRIBUTION OF THIS DOCUMENT IS UNLIMITED

NOV 0 4 1991

INTRODUCTION

Compared to the photon dosimetry, neutron dosimetry is more complicated. This paper summarizes in detail a large portion of the experimental work on neutron dosimetry that has been done at SLAC. First, the dosimetric characteristics of the five radioisotopic type neutron sources (^{238}PuBe, ^{252}Cf, ^{238}PuB, $^{238}PuF_4$ and ^{238}PuLi) are introduced. The mass numbers of the neutron sources will be omitted in the following text. Then, the neutron instrumentation that are commonly in use at SLAC (moderated BF_3 detector, Anderson-Braun (AB) detector, AB remmeter, Victoreen 488 Neutron Survey Meter, Beam Shut-Off Ionization Chamber (BSOIC), ^{12}C plastic scintillator detector, moderated indium foil detector, and moderated and bare TLDs) are described. This report emphasizes how the sources and instruments are used at SLAC, and the instrument energy responses. This report also provides the basic information that is useful in using the sources and the instruments.

NEUTRON SOURCES

There are five types of radioisotopic neutron sources that are commonly used at SLAC to irradiate dosimeters, to calibrate instruments, and to verify the shielding. This section describes the traceability and the dosimetric parameters of six neutron sources: large PuBe (MRC-426), small PuBe (MRC-425), Cf, PuB, PuF_4 and PuLi (in the order of decreasing average energy of source).

Traceability

The neutron emission rates of all sources shown in Table 1 are traceable indirectly back to the standards at the National Institute of Standards and Technology (NIST). The PuBe sources were calibrated by the manufacturer, Monsanto Research Corporation, against another PuBe source calibrated by NIST[1]. The Cf source was

calibrated by Savannah River Laboratory agianst a Cf source calibrated by NIST[2]. The PuB source was calibrated against a NIST-calibrated PuBe source, and the calibration result was modified by McCall[3]. The PuLi source was calibrated against two standard PuLi sources at Lawrence Berkeley Laboratory and Lawrence Livermore National Laboratory, and the mean result was used[4]. The PuF source was calibrated against the SLAC PuLi source[3]. Uncertainty values for the neutron emission rates were also given in the source calibration documents.

Dosimetric Parameters

Table 1 also shows the dosimetric parameters of the neutron sources. The average energy is the fluence-weighted average energy, and these average energy values were recommended by McCall[3]. The most detailed spectra available to the authors for all sources are shown in Figure 1 for PuBe[5], in Figure 2 for Cf[6], in Figure 3 for ^{241}AmB[7] (spectrum of PuB is assumed to be the same), in Figure 4 for PuF$_4$[8] and in Figure 5 for PuLi[9]. The spectra in Figures 1-5 were calculated and/or measured for sources of a specific size and, therefore, the spectra for the neutron sources at SLAC may be slightly different from the spectra shown in Figures 1-5. However, these reference spectra are still very useful for the interpretation of the energy response of a dosimeter or an instrument after the energy response calibration.

The half-life is 87.74 *y* for a Pu-related source and is 2.64 *y* for Cf. The ^{241}Pu impurity in the Pu-related source decays into ^{241}Am, and this phenomenon may change the effective half-life of a Pu-related source. A good illustration for this effect can be seen in Reference 10. However, this effect is neglected in the half-life determination for the ^{238}Pu-related sources at SLAC, because the oldest source (PuLi) at SLAC is only 27 years old since it was manufactured.

The neutron emission rates on 5-1-90 for the sources were derived from the source calibration information by simply accounting for the decay between 5-1-90 and the source calibration dates. The uncertainty value for each source is also shown in percentage in Table 1.

The anisotropic factor is the ratio of the fluence from the true source to the fluence from an isotropic source. The anisotropic factor given here should be applied when, during source irradiation, the detector is at a point on a line perpendicular to the vertical axis of the source. The anisotropic factors for all sources were measured by McCall[11], except that for Cf was measured by Ipe[12].

The fluence-to-dose equivalent conversion factors (h_ϕ in units of rem cm^2) for the sources were obtained from Figure 31(a) of the National Council on Radiation Protection and Measurements Report No. 79 (NCRP79)[13], except that for the Cf source was obtained from Reference 14. For comparison purposes, the International Commision on Radiological Protection (ICRP) Publication 21[15] spectrum-averaged fluence-to-dose equivalent conversion factor for the PuBe spectrum in Figure 1 is 3.7×10^{-8} rem cm^2, which is close to the value of 3.64×10^{-8} rem cm^2 for the PuBe in Table 1.

Table 2 shows the fluence rates (ϕ) and dose equivalent rates (H) on 5-1-90 for the five neutron sources at SLAC for the source-to-detector distances of 0.5 m and 1 m. The height for both the detector and source is 152 cm for the Pu-related sources, and 162 cm for the Cf source. Table 2 serves as an easy and quick reference for source users who only need to take into account the source decay during his/her instrument calibration.

The direct fluence rate (ϕ_d in units of cm^{-2} s^{-1}) and the direct dose equivalent rate (H_d in units of mrem h^{-1}) for each source are derived by the following equations:

$$\phi_d = NF/4\pi r^2 \tag{1}$$

$$H_d = 3.6 \times 10^6 \, \phi_d \, h_\phi \tag{2}$$

where

N = Neutron emission rate for source in s^{-1}.

F = Anisotropic Factor.

r = Source-to-detector distance in cm.

h_ϕ = Fluence-to-dose equivalent conversion factor in Table 1.

The scattered/direct fluence ratio ($f_\phi = \phi_s/\phi_d$) and the scattered/direct dose equivalent ratio ($f_H = H_s/H_d$) for the source in the single ground plane scattering situation can be estimated with Jenkins' recipes[16] as follows:

$$f_\phi = \frac{1.52\, r_i/r}{(1 + 0.1\, E_{av}) \left(1 + \left(\frac{r_i}{r}\right)^3\right)} \tag{3}$$

$$f_H = \frac{0.75\, r_i/r}{\left(1 + \left(\frac{r_i}{r}\right)^3\right)} \tag{4}$$

where

r_i = Image source-to-detector distance in cm.

r = Source-to-detector distance in cm.

E_{av} = Source average energy in MeV.

Note that f_ϕ is a function of the source's average energy and f_H is independent of the source. The error of f_ϕ and f_H from Jenkins' method is ~10%.

For the Cf source in the single ground plane scattering situation, Schwartz[14] gave the following equations to estimate the scattering more accurately:

$$f_\phi = 2.16\, h r^2\, r_i^{-3} \tag{5}$$

$$f_H = 0.8\, h r^2\, r_i^{-3} \tag{6}$$

where

h = Height for source in cm.

r and r_i = Same as those in Equations (3) and (4).

The f_ϕ and f_H values for the Pu-related soruces in Table 2 were estimated using Jenkins' recipes and those for Cf were estimated using Schwarz' formula.

It has been demonstrated[17] that both the scattering estimation methods of Jenkins' and Schwartz' agree with the measurement results, as long as r is smaller than h. The Schwartz method gave a f_H value of 0.9% and 3.3% at 0.5 m and 1 m, respectively, for the Cf source. Jenkins' formula [Equation (4)] would give a f_H value of 2% and 7% at 0.5 m and 1 m, respectively, for the Cf source. These values are the same for all other sources, since the f_H value is not a function of E_{av}.

The total fluence rate and the total dose equivalent rate are simply the summation of the scattering component and the direct component. It is generally desired to keep the scattering component as small as possible during the calibration of an instrument or dosimeter. However, at very close distance, nonuniform irradiation of an instrument may occur. Therefore, the most appropriate calibration distance between the source and detector is 50-100 cm and the height for both detector and source is ~150 cm.

INSTRUMENTATION

This section first describes five types of active instruments (moderated BF_3 detector, AB detector, AB remmeter, Victoreen 488 Neutron Survey Meter and Beam Shut Off Ionization Chamber) and then three passive instruments (^{12}C plastic scintillator detector, moderated indium foil detector, and moderated and bare TLDs). Emphasis is given to the energy response and the usage of the instrument.

Moderated BF_3 Detector and AB Detector

The moderated BF_3 detector and AB detector are specially designed and made to be used in an accelerator facility to measure neutron fluence rate and dose equivalent rate, respectively. Three major characteristics of the instruments: energy and angular responses, usage and dead time correction, are described as follows.

Energy and angular responses

A schematic drawing of the SLAC-made moderated BF_3 detector (based on an early LBL design) is shown in Figure 6. The BF_3 proportional counter (Reuter Stokes RS P1 1613; 5 cm diameter and 33 cm long) with an attached preamplifier is inserted into the Cd-covered cylindrical polyethylene moderator (radial thickness 6 cm) to form the moderated BF_3 detector. The moderated BF_3 detector is designed to have an energy-independent fluence response over a wide range of neutron energy. The calculated energy response functions of a moderated BF_3 detector by Kosako et al.[18] are reproduced in Figure 7. Although the sensitive volume of their BF_3 counter is only 11% of ours, the 6 cm radial thickness of the polyethylene moderator, which dominates the energy response of the detector, is the same. Therefore, the energy dependence of the SLAC moderated BF_3 detector should be very similar to that in Figure 7.

When neutrons incident from the lateral side of the detector, the response (in units of counts cm^2) is flat from 10 eV to 10 keV and rises to a peak at 1 MeV and then drops sharply after 10 MeV. When neutrons incident from the end, the response shape is similar but the response is only 10% of the response for lateral incidence (peak response also shifts to 5 MeV). This indicates that, in field or calibration measurements, the lateral side of the detector has to face the source direction. Also because of the large detector size, uniform irradiation of the whole detector volume has to be noted during measurements

A schematic drawing of an Anderson-Braun (AB) BF_3 detector[19] is shown in Figure 8. The SLAC-made AB detector has the same specification as that in Figure 8. The energy response of the AB detector is tailored to be close to the fluence-to-dose equivalent conversion factor curve, through the use of an appropriate polyethylene moderator thickness and the imbeded boron plastic absorber which has a certain number of holes. The AB detector is, therefore, designed to measure the neutron dose equivalent directly. The dose equivalent response curve of the AB detector obtained from References 20–22 is shown in Figure 9. The AB detector has a higher response to lower energy neutrons than to high energy neutrons, and the response drops sharply after 10 MeV. If the AB detector is calibrated against Cf, it would respond by 10% low for AmBe or PuBe, ~50% low for 14 MeV neutrons and high for low energy neutrons (e.g., PuLi). Due to its pseudo-spherical body, the AB detector has similar responses for neutrons incident from the side and that from the end. However, the response of the AB detector for neutrons incident from the head (i.e., from the electronic side) is only 20–50% of that from the side, depending on the source energy.

Usage

The moderated BF_3 detector and the AB detector are generally used in combination at SLAC (BF_3 detector measures fluence rate and AB detector measures dose equivalent rate) so that the average energy of the neutron spectrum may be estimated. Figure 10 shows the electronic set-up of the moderated BF_3 and the AB detectors, as well as the settings for the parameters [e.g., high voltage, gain (C × F is coarse × fine), input, output, etc.].

A high voltage of 2190–2200 V for both the detectors was obtained by establishing the high voltage characteristic curve for each detector (counting rate vs. high voltage). A plateau region can be found for each characteristic curve. The plateau for the moderated BF_3 and the AB detectors have the slopes of 1.2%/100 V and 2.5%/100 V, respectively. The high voltage was chosen to be the midpoint of the plateau.

Figure 11 shows the typical discriminator voltage counting curves (counting rate vs. discriminator voltage of the Counter & Timer) of the moderated BF_3 and AB detectors to $^{238}PuBe$ with no photon pile-up. These curves need to be established, and are used to decide the neutron counting efficiencies for different discriminator voltage settings (higher voltage setting is used to reject the photon pile-up signals in a field with high photon intensity). For example, the extrapolation point to a discriminator setting of zero volts for the AB detector (see the dashed curve in Figure 11) is ~95 cps, which is equivalent to 100% counting efficiency. If a discriminator voltage of 4 V is required to reject the photon pile-up signals in a mixed field with high photon intensity (can be seen with an oscilloscope), the neutron counting efficiency at 4 V will be (88/95) = 93%. Figure 11 also shows that a discriminator setting of 1.5–2 V can achieve a counting efficiency close to 100% in a field with low photon intensity

(therefore small pile-up). The background counting rates for the moderated BF_3 and AB detectors at a discriminator voltage of 2 V are 6 cpm and 1 cpm, respectively.

Table 3 summarizes the neutron response calibration results for the moderated BF_3 detector and AB detector at SLAC using radioisotopic neutron sources. The optimum response values of the detectors for GRN are the values that the authors recommend to be used in the accelerator field measurements for the giant resonance neutrons (GRN), based on the consideration of the detector's energy response, neutron spectra and the estimated errors of the calibration. The fluence-to-dose equivalent conversion factor used at SLAC for GRN is 3.18×10^{-8} rem cm^2. The optimum response values of the moderated BF_3 and AB detectors for GRN are 14.5 counts cm^2 and 7000 counts mrem^{-1}, respectively.

A detailed description of the detection theory and operation procedure for the moderated BF_3 detector can be seen in Reference 23.

Dead time correction

Dead time effect on the response of a pulse detector has to be considered especially in an accelerator field. The dead time correction for a pulse detector with a dead time of T_d in a continuous field is well known, and can be expressed as Equation (7) when using a nonparalysable model[24]:

$$R_t = \frac{R}{1 - RT_d} \tag{7}$$

where

R_t = True counting rate (counts s^{-1}).

R = Measured counting rate (counts s^{-1}).

T_d = Dead time of detector (s).

In a pulse field such as that in accelerator facilities, the duty factor of the beam pulse would affect the dead time effect in the following ways[25]. If the beam pulse length T_p is longer than the dead time T_d, then

$$R_t = \frac{R}{1 - \frac{RT_d}{PT_p}\left(1 - \frac{1}{2}\frac{T_d}{T_p}\right)} \tag{8}$$

where

P = Pulse repetition rate (number of beam pulse per second).

PT_p = Duty factor.

If the pulse length T_p is shorter than the dead time T_d, then

$$R_t = R - P\ln\left(1 - \frac{R}{P}\right) \tag{9}$$

Most accelerator beams have a pulse length T_p that is shorter than 1 μs and most health physics neutron instruments have dead time T_d about a few microseconds. Therefore, Equation (9) should be applied in that case. However, for a moderating type detector using a thermal neutron sensor, the moderation time (the time for a fast neutron to slow down in the moderator to become a thermal neutron, and to reach the sensor) also play a role in affecting the dead time correction. Due to the moderation, the short burst of neutrons from a beam pluse is stretched over a longer period of time to be detected by the sensor. Therefore, for the thermal neutron sensor, the "effective" beam pulse length is determined by the moderation time, not by the physical beam pulse length T_p. Because of this and the fact that the moderation time

is generally around hundreds of microseconds (much longer than T_d), we can replace T_p with T_m (mean moderation time) in Equation (8) and establish Equation (10):

$$R_t = \frac{R}{1 - \frac{RT_d}{PT_m}\left(1 - \frac{1}{2}\frac{T_d}{T_m}\right)} \tag{10}$$

The T_m/T_d values for the moderated BF_3 and the AB detectors were measured to be about 73 and 14, respectively[26]. In this case, the parenthetical term in Equation (10) can be neglected in this case with small error, and Equation (10) then becomes Equation (11).

$$R_t = \frac{R}{1 - \frac{R}{P}\frac{T_d}{T_m}} = \frac{Rr}{r-1} \tag{11}$$

where

$$r = \frac{PT_m}{RT_d}$$

The parameter r is the ratio of the maximum counting rate that can be measured (PT_m/T_d) to the measured counting rate (R). Therefore, r cannot be smaller than one.

Equation (11) was used by Jenkins for the dead time correction for the moderating type detectors measuring neutrons in a pulse field[27]. Equation (11) was derived based on the assumption that the thermal neutrons detected by the sensor are uniformly distributed in time T_m after each beam pulse and, therefore, a mean moderation time T_m is used. According to Jenkins[28] and Dinter's[29] measurements, however, the neutron signals recorded in the sensor are roughly distributed exponentially, not uniformly. If the paralysable model[24] and the exponential distribution of neutron

signals are used, the dead time correction for a moderating type detector in a pulse field would be[26]

$$R_t = R\,r \ln \frac{r}{r-1} \qquad (12)$$

where r is the same as that in Equation (11).

The dead time corrections for the moderated BF_3 and the AB detectors in pulse fields with pulse repetition rates of 10 pps and 180 pps are shown in Figure 12. The correction factor, $F = R_t/R$ from Equation (11) (nonpara model) or Equation (12) (para model), is to be multiplied to the measured counting rate R to obtain the true counting rate R_t. A correction factor of two indicates a dead time counting loss of 50%. It can be seen from Figure 12 that:

(1) Due to its higher T_m/T_d value, the moderated BF_3 detector has a lower dead time counting loss compared to the AB detector for the same measured counting rate. However, due to the much high detection efficiency of the moderated BF_3 detector (a factor of ~70 higher than the AB detector) the moderated BF_3 detector has a larger dead time counting loss (i.e., larger F) than the AB detector in the same field.

(2) The lower the pulse repetition rate P, the smaller the r and the larger the correction factor F. The dead time correction of a detector operated in a pulse field is obviously much more significant than that operated in a continuous field.

(3) The correction factor predicted with the paralysable model is smaller than that with the nonparaysable model. Ash et al.[26] demonstrated that Equation (12) (para) is more suitable than Equation (11) (nonpara) to describe the dead time correction of the moderated BF_3 and AB detectors.

Dinter and Tesch[29] have measured the moderation times and calculated the dead time corrections for four common moderating type remmeters. Their results for the

AB remmeter are reproduced in Figure 13 (note that they used different symbols than ours). The counting loss factor C in Figure 13 is the inverse of the correction factor F in Figure 12 (i.e., $C = 1/F$). Because the factor C becomes independent of the pulse width Lp for Lp less than 10 μs, the result for 1 μs pulse length is applicable to the narrow beam pulses that are common to most accelerator facilities.

The way to use Figure 13 is illustrated in the following example (also see the arrows in Figure 13): in a field with a true dose equivalent rate (D) of 10 mrem h^{-1}, an AB remmeter in a pulse field of 10 pulses per second and a pulse length (L_p) of 1 μs would have a counting-loss factor of 96%. Since the true dose equivalent rate (generally unknown) is used, Figure 13 is not as useful in estimating the needed dead time correction for an AB remmeter used in an unknown field.

A comparison of the dead time correction for the AB detector predicted with Figures 12 and 13 is made below. The SLAC AB detector has a sensitivity of 1.8 cps per mrem h^{-1} for ^{238}PuBe. The above-mentioned field of 10 mrem h^{-1} would result in the reading of an AB remmeter to be 9.6 mrem h^{-1} (because C = 0.96) according to Figure 13. This is equivalent to a measured counting rate of $1.8 \times 9.6 = 17$ cps for the AB detector. Using paralysable model, 17 cps should give an F factor of ~1.07 according to Figure 12 [or Equation (12)], which is larger than $1/C = 1.04$. Therefore, the dead time correction for the AB detector (or remmeter) predicted from Figure 13 is smaller than that predicted from the paralysable model in Figure 12. The larger the counting rate (i.e., the field intensity), the larger the difference will be.

The importance of the dead time correction can be shown in the following example. In a field of 1 mrem h^{-1} and 10 pps, the dead time correction factor is ~1 for an AB detector (or remmeter) but is 1.1 for the moderated BF_3 detector having a sensitivity of 120 cps per mrem h^{-1}. In a field of 5 mrem h^{-1} and 10 pps, the corre-

sponding correction factor is 1.04 for an AB detector and is 2.08 for the moderated BF_3 detector.

AB Remmeter

The SLAC AB remmeter, similar to the commercially available SNOOPY remmeter[22], has a detector design the same as that in Figure 8 and an attached electronic part that is calibrated to read the neutron dose equivalent rate directly. Therefore, the AB remmeter should have very similar energy response (see Figure 9) and dead time correction (see Figures 12 and 13) as those of the AB detector. The response calibration results of the AB remmeter are also shown in Table 3.

Victoreen 488 Neutron Survey Meter

Victoreen Model 488 neutron survey meter is a portable meter similar to the Eberline 9-inch sphere remmeter instrument. It consists of a boron-lined proportional counter (1-inch diameter and 6 inches long) which can be inserted into a cylindrical polyethylene moderator (3-inch diameter and 7.5 inches long with a cavity for the counter). Because the moderator thickness is only about one inch, the meter is much lighter but the neutron energy response is also much poorer than those of AB remmeter. The meter is designed to measure neutrons with energy less than 10 MeV. The meter-head is calibrated to read cpm for fast neutron measurement when the counter is inside the moderator, and to read thermal neutron fluence rate in units of $cm^{-2}\ s^{-1}$ with bare counter only.

Due to its cylindrical shape, the response of the meter is directional-dependent. The lateral side of the meter should be toward the radiation source during measurement or calibration. The calibration results of the fast neutron response of the Victoreen 488 Neutron Survey Meter are shown in Table 3. The optimun response

value of the meter to GRN is 100 cpm per mrem h^{-1}(±20%). The dead time effect of the meter operated in a pulse field is not known.

Beam Shut-Off Ionization Chamber (BSOIC)

The SLAC-made BSOIC is a special type of tissue-equivalent ionization chamber used to monitor continuously the radiation levels outside the SLAC beam facilities and trip the beam off automatically if the presetted tripping level is exceeded. A BSOIC consists of a ten-liter aluminum cylinder (~24 cm diameter and ~24 cm high) filled with one-atm ethane (C_2H_6), which sits on top of the electronic and display components. A small ^{90}Sr-Y source is fixed inside the cylinder to act as a continuous internal check source so that it can be sure that the BSOIC is working. The detector has roughly equal rad responses to photons and fast neutrons on an equal rad dose basis. Since the radiation fields in SLAC (an electron accelerator facility) are dominated by photons, the BSOIC is adjusted to readout photon exposure rate in units of mR h^{-1}.

The dose equivalent response of the BSOIC to neutrons is also shown in Table 3. The optimum response value of BSOIC to GRN is ~ 0.12 mR h^{-1} per mrem h^{-1}. In a field with an equal amount of photon and neutron dose equivalent rate, neutrons will contribute about 10% of the total response only. With a high voltage of 500 volts, the collection efficiency of the BSOIC is higher than 95% in a pulse field of 10 pps and an average photon intensity less than 1 R h^{-1}.

^{12}C Plastic Scintillator Detector

The ^{12}C plastic scintillator detector is a threshold detector used to measure high energy neutrons (> 20 MeV) in accelerator fields. The detection principle and usage of the ^{12}C scintillator detector are described as follows.

Principle

The neutrons in an electron accelerator facility come from the giant resonance, pseudo-deuteron and photopion interactions of the photons with materials. Therefore, the neutrons have energies covering from thermal up to a maximum energy that equals to the electron beam energy. The response function of the SLAC moderating type detectors (see Figures 7 and 9) show that the detectors have very low responses to neutrons above 10–20 MeV (i.e., they measure mainly the giant resonance neutrons). In order to measure the high energy neutrons above 20 MeV, the ^{12}C plastic scintillator detector introduced by McCaslin[30] is used at SLAC. The carbon nuclei (^{12}C) in a plastic scintillator have the ^{12}C $(n,2n)^{11}$C reaction when interacting with high energy neutrons. The cross section of the ^{12}C $(n,2n)^{11}$C reaction[30–32] shown in Figure 14 has a lower neutron threshold at ~20 MeV, and the cross section rises rapidly and becomes flat at ~22 mb for neutrons above 30 MeV. An effective cross section of 22 mb is generally used for this reaction to determine the nominal neutron fluence above 20 MeV.

Figure 14 also shows a possible interfering reaction, ^{12}C $(\gamma,n)^{11}$C, that is important in electron accelerator facilities.‡ The ^{12}C $(\gamma,n)^{11}$C reaction has a peak at ~24 MeV photons[33]. It is not easy to determine the fractions of gammas and neutrons that are above 20 MeV in a field. Therefore, to eliminate this high energy gamma interference, the ^{12}C plastic scintillator detector should be used outside a thick (e.g., 2 or 3 feet) concrete shield where gamma/neutron ratio is not too large, or a lead brick shielding (1 TVL = 3 cm for 24 MeV gammas) should be used between the detector and the radiation source to attenuate the gammas.

‡ In a proton accelerator, the interfering reactions are the ^{12}C$(p,d)^{11}$C and ^{12}C$(\pi,\pi n)^{11}$C reactions.

Usage

The ^{12}C plastic scintillator detector is basically an activation detector. The ^{11}C product is a pure β^+ emitter (E_β = 0.98 MeV) and has a half-life of 20.4 min. A ^{12}C scintillator (5-in dia. and 5-in height, 1720 gm) is put in the field for exposure (activation), and then brought back to the laboratory, and the ^{11}C activity is counted as that shown in Figure 15 as soon as possible. The settings of the instruments' parameters, e.g., high voltage, gain and shape time, are also shown in Figure 15. The lead shielding covered with a black cloth is to reduce the background and light noise. A layer of mineral oil between the unpainted side of the scintillator and the photomultiplier tube is used to create a better scintillation light transmission.

Assuming a plastic scintillator has been exposed in a field for t_i minutes, the decay time between the end of exposure and the start of the counting is t_d minutes and the counting period is t_c minutes, the following equation is used to determine the saturation activitiy A_s dpm:

$$A_s = \frac{\lambda(G - Bt_c)}{\left[e^{-\lambda t_i} - e^{-\lambda(t_d+t_c)}\right]\left(1 - e^{-\lambda t_i}\right) f} \tag{13}$$

where

λ = Decay constant of ^{11}C = 0.693/20.4 min = 0.034 min^{-1}.

G = Gross counts at a discriminator voltage of 2 V.

B = Background counting rate at a discriminator voltage of 2 V = 13 cps.

f = Detection efficiency (cpm/dpm) = 1.

A conversion constant of 104 dpm/(n/cm^{2}s)[30] is used to convert the saturation activity A_s to the neutron fluence rate above 20 MeV. The neutron spectrum above 20 MeV for an electron accelerator may be assumed to be the same as that for a

proton accelerator, based on the equilibrium spectrum concept. Therefore, a fluence-to-dose equivalent conversion factor of 28 fSv m^2 for the neutron spectrum outside the shielding of a proton accelerator[32] can be used at SLAC to relate the fluence rate to the dose equivalent rate for neutrons above 20 MeV.

The conversion constant of 104 dpm/$(n/cm^2\ s)$ is calculated based on the assumption that the scintillator is exposed to high energy neutrons uniformly over the detector volume and is activated with an effective cross section of 22 mb. Under the same assumption, the ^{11}C activity should also be uniform inside detector. Therefore, this ^{11}C scintillator counting system is basically a 4π counting system and the detection efficiency f in Equation (13) is 1, if the counting efficiency is 100% (i.e., ^{11}C activity is measured at zero discriminator voltage).

However, due to the large background noise signals that will be counted, the ^{11}C activity cannot be measured at zero discriminator voltage. Because the energy per decay of ^{60}Co (1.17 and 1.33 MeV photons) is similar to that of ^{11}C (0.98 MeV positron and two 0.511 MeV photons), the discriminator voltage counting curves for ^{60}Co and ^{137}Cs and the background counting curve in Figure 16 can be first established to facilitate the ^{11}C counting. The discriminator curve for ^{60}Co or ^{137}Cs in Figure 16 is obtained by irradiating the unexposed ^{12}C scintillator detector with ^{60}Co or ^{137}Cs, using the parameter settings in Figure 15. The purpose of establishing the discriminator curve for ^{60}Co is to have the optimum settings for all parameters (gain, HV and shape time) so that the following three conditions are met: (1) the after-pulses from cosmic rays are < 0.5 V; (2) the pulses > 10 V are not much (18% in Figure 16); and (3) the extrapolated counting rate at zero discriminator voltage is not much larger than that at ~2 V (it is 110/90 = 1.22 times larger in Figure 16). The discriminator voltage curve for ^{11}C counting in Figure 16 shows that the counting

efficiency at a discriminator voltage of 2 V is ~100%. The background counting rate at 2 V is 13 cps (1 σ = 10%). These are the values used in Equation (13).

Assuming the time periods for exposure, decay and counting are all about 20 min, the detection limit of the ^{12}C scintillator detector system, using a criterion of 3 σ background (i.e., 4 cps), can be calculated with Equation (13). The lowest neutron dose equivalent level corresponding to the detection limit is 1.3 mrem h^{-1} for neutrons > 20 MeV.

A detailed detection and operation principles of the ^{12}C plastic scintillator detector and the ^{11}C counting system can be found in References 30 and 34.

Moderated Indium Foil Detector

As can be seen from the dead time corrections in Figures 12 and 13, the active detectors may not be suitable to be used in an accelerator field with a high neutron intensity and a low pulse repetition rate. The moderated indium foil detector, an activation type detector, is suitable in that case. The moderated indium foil detector was originally introduced by Stephens[35]. It was an indium foil encased in a paraffin sphere (6-in dia.) placed in a cadmium box. The SLAC moderated indium foil detector is an indium foil (4.5 cm dia., 0.01-in thick, and ~2.7 g) inside the center of a polyethylene moderating cylinder (6-in dia., 6-in height) covered with cadmium. The detector is designed to have a maximum and flat fluence energy response for neutrons between 10 keV and 10 MeV.

Incident fast neutrons moderated by the polyethylene become thermal neutrons and are absorbed by the indium foil through the $^{115}In(n,\gamma)^{116m}In$ and the $^{113}In(n,\gamma)^{114m}In$ reactions. ^{113}In has a smaller thermal neutron capture cross section (8.1 b) and a smaller abundance (4.3%) than those of ^{115}In (162.3 b and 95.7%, respectively). The half-life of ^{114m}In (49.5 d) is also longer than that of ^{116m}In

(54.2 min). Therefore, only the ^{115}In$(n,\gamma)^{116m}$In reaction is important in the neutron field measurements using the moderated indium foil detector. After an exposure time of t_i min and a decay time of t_d min, the foil is brought back to the laboratory for a counting of t_c min. Equation (13) can be used to determine the saturation activity A_s dpm of the foil, except now that λ is 0.0128 min^{-1} for the beta decay of ^{116m}In, and the parameters G, B and f are related to the ^{116m}In beta counting system.

The GM counting system of Radiation Physics Dept. is used to measure the indium foil activity. The stability of the GM system is maintained with a small ^{36}Cl beta disk source (30 nCi on 11-01-86) to have a counting rate of 569 cps when the source is counted on the third shelf from the top. The instrument settings are 1000 volt high voltage and 0.5 V discriminator voltage.

The background counting rate B of an unexposed indium foil is 21 cpm (1 σ = 17%). The detection efficiency f is not used and, therefore, the neutron fluence rate (cm^{-2} s^{-1}) is related directly with the specific saturation counting rate (cpm g^{-1}) under the condition that the stability of the GM system is maintained to be constant.

Figure 17 shows the sensitivity (cpm g^{-1} per n/cm^2 s) vs. neutron energy for the moderated indium foil detector from the calibration works at SLAC and by Stephens[35]. The moderator thickness is 6-in for both types of detectors and, therefore, they should have similar relative energy response. The Stephens' results are scaled to SLAC's ^{252}Cf result in Figure 17. The optimum sensitivity value for the GRN is ~3 cpm g^{-1} per n/cm^2 s. Assuming the t_i, t_d and t_c are all 20 min, the lowest neutron dose equivalent level corresponding to the detection limit (3 σ background criterion) for the moderated indium foil detector is 1 mrem h^{-1} of GRN. The response of the moderated indium foil detector for neutrons incident from the end (parallel to detector axis) is lower than that from the side by no larger than 10%.

Both the ^{12}C plastic scintillator detector and the moderated indium foil detector are passive activation type detectors and are free from dead time effect. Due to their short half-lives (20.4 min for ^{11}C and 54.2 min for ^{116m}In), they are suitable to be used in combination for short-term (e.g., 30 min) field measurements of high (> 20 MeV) and fast (< 20 MeV) neutrons, respectively, if the field intensity is stable during the measurement period. For long-term low intensity environmental neutron monitoring, both the active instrument (moderated BF_3 detector) and the moderated TLD (described below) are used at SLAC.

Moderated and Bare TLDs

The moderated TLD has the same design as the moderated indium foil detector, except that the indium foil is replaced with a ^{6}LiF/^{7}LiF pair (the ^{6}LiF and ^{7}LiF are LiF teflon disk). The signal of the ^{7}LiF element is used to estimate the photon signal of its paired ^{6}LiF element. The net neutron signal of the ^{6}LiF element is then used to derive the neutron fluence (or dose equivalent). The moderated TLD is designed for the same purpose as that of the moderated indium foil detector, i.e., a high and flat fluence response for neutrons between 10 keV and 10 MeV, and a nearly isotropic response. However, TLDs do not decay and have a lower sensitivity and, therefore, the moderated TLD is suitable for long-term (months) low intensity neutron field monitoring.

Figures 18 and 19 show the neutron sensitivity of the moderated ^{6}LiF TLD to five neutron sources at SLAC in units of V Sv^{-1} and V cm^2, respectively (see the curves with triangle points). These curves are given for the bare TLD with a sensitivity of 1 V rad^{-1} to ^{137}Cs gammas (the TL light output is in units of volts at SLAC). A pair of ^{6}LiF/^{7}LiF is also generally put on the outer surface of the moderator so that the incident thermal neutrons can be measured. The calibration results for the

^{6}LiF TLD on the surface of the moderator are also shown as the curves with open circle points in Figures 18 and 19. It is clear that the fluence responses (Figure 19) of the ^{6}LiF TLDs inside and outside the moderators are more energy-independent than their dose equivalent responses (Figure 18). The ^{6}LiF TLD outside the moderator also has a much smaller sensitivity (a factor of ~15) than that inside the moderator for SLAC sources. The fluence sensitivity of the moderated ^{6}LiF TLD for GRN estimated from Figure 19 is 6.7×10^{-8} V cm^2. The corresponding dose equivalent sensitivity is 210 V Sv^{-1}(2.1 V rem^{-1}). Because the TL output is expressed in terms of the photomultiplier output, the stability of the TLD light counting system must be maintained with the light source.

Personnel neutron TLD

Figures 18 and 19 also show the sensitivity of the ^{6}LiF TLD on the surface of the SLAC water phantom (see the solid circle points). This is similar to the situation that a TLD is worn by a person and, therefore, the calibration results of the TLD on a water phantom in Figures 18 and 19 can be used to estimate the personnel neutron dose equivalent from the personnel TLD monitoring result. Again the fluence response of the ^{6}LiF on a water phantom is more energy-independent than its dose equivalent response. The fluence sensitivity of the ^{6}LiF on a water phantom for GRN estimated from Figure 19 is 2.2×10^{-8} V cm^2. The corresponding dose equivalent sensitivity is 69 V Sv^{-1} (0.69 V rem^{-1}).

The difference between the ^{6}LiF TLDs on a water phantom and on a moderator is that there is a cadmium sheet in the moderator to absorb the albedo neutrons in the moderator. Therefore, the ^{6}LiF TLD on a water phantom has a higher response (a factor of 2.4) than that on a moderator. The ^{6}LiF TLD on a water phantom

measures incident fast neutrons through albedo neutrons, while the ^{6}LiF TLD on a moderator measures only the incident thermal neutrons.

The ^{6}LiF TLD outside the moderator has a thermal neutron sensitivity of 150 V rem^{-1} (1.7×10^{-7} V cm^2), according to Jenkins' TLD wallet calibration results. Because there is no cadmium in the front of the TLD on a water phantom, the incident thermal neutrons in the field would increase the response of the ^{6}LiF TLD. Jenkins[36] has studied the sensitivity of the ^{6}LiF TLD on a water phantom as a function of the fast/thermal neutron fluence ratio in the SLAC fields. It is obvious that the smaller the fast/thermal ratio, the larger the sensitivity will be. The above-mentioned dose equivalent sensitivity of 0.69 V rem^{-1} is corresponding to the TLD result in a field with a fast/thermal ratio of ~13 (i.e., 7% thermal fluence in the field). Jenkins also suggested[36] that, for a typical SLAC field, the most likely fast/thermal ratio is 2.75, and the corresponding dose equivalent sensitivity is 300 V Sv^{-1} (3 V rem^{-1}).

SUMMARY AND CONCLUSIONS

A detailed description and summary of the neutron dosimetric work at SLAC (neutron sources and instrumentation) are given in this report. With the comprehensive information and calibration results covered, this report is aimed to be used as a reference and guide.

REFERENCES

1. Monsanto Research Corporation. "Shipping Data Form for the Neutron Source" (1971).

2. Savannah River Laboratory. "Information Sheet for Neutron Source" (1981).

3. R. C. McCall, Radiation Physics Group File (Aug. 5, 1988).

4. R. C. McCall, Radiation Physics Group File (Jun. 18, 1985).

5. S. Block, J. Bryan, C. Prevo and D. Montan, "Laboratory Sources Enhanced 0.5 eV to 200 keV Neutrons for Instrument Evaluation," Health Phys. **13**, pp. 1025-1031 (1967).

6. International Atomic Energy Agency. *Neutron Monitoring for Radiological Protection*. Vienna:IAEA; IAEA Technical Report Series No. 252 (1985).

7. E. A. Lorch, Int. J. Appl. Radiat. Isotopes, **24**, pp. 585 (1973).

8. O. P. Massand and G. Venkataraman, "The Neutron Spectrum of Plutonium Fluoride," Nucl. Instrum. and Meth., **121**, pp. 405-406 (1974).

9. H. Ing, Personal Communication to R. C. McCall, Chalk River Nuclear Laboratories, Canada (1982). Also, H. Ing., W. G. Cross and B. J. Tymons, "The Spectrum of Neutrons from a ^{238}PuLi Sources," Health Phys., **40**, pp. 345-350 (1981).

10. K. J. Ellis, "The Effective Half-life of a Broad Beam ^{238}PuBe Total Body Neutron Irradiator," Phys. Med. Biol., **35**(8), pp. 1079-1088 (1990).

11. R. C. McCall, Radiation Physics Group File (Jul. 1981).

12. N. E. Ipe, *Radiation Physics Notebook BD* and *CR-39 Book No. 3*, p. 85 (1987).

13. National Council on Radiation Protection and Measurements, *Neutron Contamination from Medical Electron Accelerators*, NCRP Report No. 79 (1984).

14. R. B. Schwartz and C. M. Eisenhauer, "Procedures for Calibrating Neutron Personnel Dosimeters," *NBS* Special Publication 633 (1982).

15. International Commission on Radiological Protection. *Data for Protection Against Ionizing Radiation for External Sources*, Oxford Pergamon Press; ICRP Publication 21 (1973).

16. T. M. Jenkins, "Simple Recipies for Ground Scattering in Neutron Detector Calibration," Health Phys., **39**, pp. 41-47 (1980).

17. J. C. Liu, C. S. Sims, W. H. Casson, H. Murakami and C. Francis, "Neutron Scattering in ORNL's Calibration Facility," Radiat. Prot. Dosim., **35**, pp. 13-21 (1991).

18. T. Kosako, T. Nakamura and S. Iwai, "Estimation of Response Functions of Moderating Type Neutron Detectors by the Time-of-Flight Method Combined with A Large Lead Pile," Nucl. Instrum. Methods in Phys. Res., **A235**, pp. 103-122 (1985).

19. H. W. Patterson and R. H. Thomas, *Accelerator Health Physics*, Ch. 5, p. 268, Academic Press Inc, New York, NY (1973).

20. F. M. Cummings, G. W. R. Endres and L. W. Brackenbush, "Neutron Dosimetry at Commercial Nuclear Plants," NUREG/CR-2956, PNL-4471 (1983).

21. E. Piesch, B. Burgkhardt and I. Hofmann, "Calibration of Neutron Detectors in Radiation Protection," Kernforschungszentrum, Karlsruhe, KfK-2847 (1979).

22. D. E. Hankins and Cortez, J. R., "Energy-Dependence of Four Neutron Rem-meter Instruments," Health Phys. **82**, pp. 305-307 (1975).

23. H. W. Patterson and R. H. Thomas, *Accelerator Health Physics Appendix-Laboratory Manual*, pp. 595-600, Academic Press, Inc., New York, NY (1973).

24. G. F. Knoll, *Radiation Detection and Measurement*, Ch. 4, p. 121, John Wiley & Sons, Inc. 2nd Edition (1989).

25. H. W. Patterson and R. H. Thomas, *Accelerator Health Physics*, Ch 5, p. 237, Academic Press, Inc. New York, NY (1973).

26. W. Ash, H. DeStaebler, J. Harris, T. Jenkins and J. Murray, "PEP Radiation Shielding Tests in SLAC A Beam," SLAC-TN-77-5, PEP-252, Stanford Linear Accelerator Center, Stanford, CA (1977).

27. T. M. Jenkins, "Neutron and Photon Measurements Through Concrete From A 15 GeV Electron Beam on a Target– Comparison with Models and Calculations," Nucl. Instrum. Methods **159**, pp. 265–288 (1979).

28. T. M. Jenkins, "Radiation Level at the Mark IV," SLAC–HP–64–1, Stanford Linear Accelerator Center, Stanford, CA (1964).

29. H. Dinter and Tesch, K. "Moderated Rem Meters in Pulsed Neutron Fields," Nuc. Instrum. Methods. **136**, pp. 389–392 (1976).

30. J. B. McCaslin, "A High-Energy Neutron-Flux Detector," Health Phys. **2**, pp. 399–407 (1960).

31. D. I. Garber and R. R. Kinsey, "Neutron Cross Sections, Vol. II Curves," Brookhaven National Laboatory, II, BNL–325, p. 30, 3rd edition (1976).

32. G. R. Steveson, "The Estimation of Dose Equivalent from the Activation of Plastic Scintillator," Health Phys. **47(6)**, pp. 837–847 (1984).

33. Berman, B. L., "Atlas of Photoneutron Cross Sections Obtained with Monoenergetic Photons," Lawrence Berkeley Laboratory, UCRL-78482, p. 9 (1976).

34. N. W. Patterson and R. H. Thomas, *Accelerator Health Physics, Appendix-Laboratory Manual*, pp. 621–626, Academic Press, Inc. New York, NY (1973).

35. L. D. Stephens and A. R. Smith, "Fast-Neutron Surveys Using Indium-Foil Activation," UCRL-8418, CA (1958).

36. T. M. Jenkins and D. D. Busick, "Personnel Dose Equivalent Monitoring at SLAC using Lithium-Fluoride TLD's," SLAC-TN-87-2 (1987).

DISCLAIMER

This report was prepared as an account of work sponsored by an agency of the United States Government. Neither the United States Government nor any agency thereof, nor any of their employees, makes any warranty, express or implied, or assumes any legal liability or responsibility for the accuracy, completeness, or usefulness of any information, apparatus, product, or process disclosed, or represents that its use would not infringe privately owned rights. Reference herein to any specific commercial product, process, or service by trade name, trademark, manufacturer, or otherwise does not necessarily constitute or imply its endorsement, recommendation, or favoring by the United States Government or any agency thereof. The views and opinions of authors expressed herein do not necessarily state or reflect those of the United States Government or any agency thereof.

Table 1. Characteristics of the radioisotopic neutron sources at SLAC.

Source	^{238}PuBe (MRC-426)	^{238}PuBe (MRC-425)	^{252}Cf	^{238}PuB	^{238}PuF$_4$	^{238}PuLi
Ave. Energy (MeV)[a]	4.2	4.2	2.2	2.1	1.5	0.5
Half-life (y)	87.74	87.74	2.64	87.74	87.74	87.74
Neutron Emission Rate (s^{-1}) on 5/1/90[b]	1.84×10^7 10%	8.90×10^5 10%	4.92×10^8 3%	3.55×10^6 15%	7.89×10^8 20%	2.27×10^6 15%
Anisotropic Factor[c]	1.09	1.06	1.11	1.08	1.07	1.07
Fluence-to-Dose Equivalent Conversion Factor (rem cm^2)[d]	3.64×10^{-8}	3.64×10^{-8}	3.33×10^{-8}	3.33×10^{-8}	2.94×10^{-8}	1.35×10^{-8}

[a] Reference 3; see Figures 1–5 for the spectra.

[b] See the traceability section in text.

[c] References 11 and 12.

[d] Derived from Reference 13.

Table 2. Fluence rates (ϕ) and dose equivalent rates (H) for the five neutron sources at SLAC on 5/1/90.

	Source	^{238}PuBe	^{252}Cf	^{238}PuB	^{238}PuF$_4$	^{238}PuLi
ϕ_d[a]	0.5 m	638	17384	122	269	77.3
(cm^{-2}s^{-1})	1 m	160	4346	30.5	67.2	19
ϕ_s/ϕ_d[b]	0.5 m	3%	2.5%	3%	3.5%	3.5%
	1 m	10%	9.0%	12%	12.5%	13.7%
ϕ[c]	0.5 m	657	17819	126	278	80.2
(cm^{-2}s^{-1})	1 m	176	4737	34.2	75.6	21.9
H_d[d]	0.5 m	83.8	2083.8	14.8	28.5	3.8
(mrem h^{-1})	1 m	20.9	520.9	3.7	7.1	0.94
H_s/H_d[e]	0.5 m	2%	0.9%	2%	2%	2%
	1 m	7%	3.3%	7%	7%	7%
H[f]	0.5 m	85.5	2103	14.9	29.1	3.9
(mrem h^{-1})	1 m	22.3	538	4.0	7.6	1.0

[a] Direct fluence rate $\phi_d = NF/4\pi r^2$, where N = neutron emission rate, F = anisotropic factor and r is the detector-to-source distance in cm.

[b] Scattered/direct fluence ratio (ϕ_s/ϕ_d) is estimated by using the recipes[16], except that of ^{252}Cf is estimated from NBS publication 633[14]. The height for both the detector and source is 152 cm (162 cm for Cf).

[c] Total fluence rate $\phi = \phi_d + \phi_s$.

[d] Direct dose equivalent rate $H_d = \phi_d h_\phi$, where h_ϕ is the fluence-to-dose equivalent conversion factor.

[e] Scattered/direct dose equivalent ratio (H_s/H_d). Same derivation method as note b.

[f] Total dose equivalent rate $H = H_d + H_s$.

Table 3. Neutron response calibration results for the four neutron sources at SLAC on 5/1/90.

	^{236}PuBe	^{238}PuB	^{238}PuF$_4$	^{239}PuLi	Optimum for GRN
Moderated	14.7	14.4	20.2	20.5	14.5
Detector (counts cm^2)	11%	15%	20%	15%	
AB Detector	6500	7600	10100	16650	7000
(counts mrem^{-1})	11%	19%	21%	19%	
AB Remmeter	0.63	0.75	0.92	1.4	0.7
(measured/true)	17%	20%	24%	18%	
Victoreen 488 Neutron Survey Meter cpm/(mrem h^{-1})	100	100	240	670	100
BSOIC (mR h^{-1})/(mrem h^{-1})	0.09	0.16	0.14	0.30	0.12

NOTE:

1. The percentage value is the estimated error. It is mainly from the error of the source strength.
2. The optimum value for GRN (giant resonance neutrons) is obtained based on the consideration of the detector's energy response, neutron spectra and the estimated errors.
3. The background counting rates for the moderated BF_3 and the AB detectors are ~6 cpm and ~1 cpm, respectively, at a discriminator voltage of 2 V.

FIGURE CAPTIONS

1. Neutron spectrum of ^{236}PuBe (drawn from the data in Blocks et. al., 1967).
2. Neutron spectrum of ^{252}Cf, normalized to a total fluence of 1 (reproduced from IAEA 1985).
3. Neutron spectrum of ^{241}AmB[7]. Spectrum of ^{238}PuB is assumed to be the same.
4. Neutron spectra of PuF_4 and AmF[8].
5. Neutron spectrum of ^{283}PuLi measured with four proportional counters[9].
6. The moderated BF_3 cylindrical detector used at SLAC.
7. Calculated energy response functions of the moderated BF_3 detector (a cylinder with a 6 cm radial thickness) for neutrons incident from the side and from the end (reproduced from Reference 18).
8. An Anderson-Braun detector[8].
9. Energy dependence of the Anderson-Braun detector (from three references).
10. The electronic set-up and parameter settings of the moderated BF_3 and AB detectors.
11. Typical discriminator voltage counting curves of the moderated BF_3 and AB detectors for ^{238}PuBe with no photon pile up. The extrapolation points at zero volts (see dashed curves) are the counting rates at 100% counting efficiency.
12. Factor F to be applied to the measured counting rate R to find the true counting rate (i.e., $R_t = RF$) for the moderated BF_3 ($T_m/T_d = 73$) and AB ($T_m/T_d = 14$) detectors operated in a pulse field. T_m and T_d are the mean moderated time and dead time, respectively. Correction factors from both the paralysable and nonparalysable models are given. A detector with a $T_d = 2\mu$s operated in a continuous field is also shown for comparison.

13. Diagram for determining the counting-loss factor C for an AB rem meter. D = true mean dose equivalent rate, D_p = dose equivalent per pulse, L_p = pulse width and f = pulse per sec.

14. Cross sections of $^{12}C(n,2n)^{11}C$ reaction[30-32] and $^{12}C(\gamma,n)^{11}C$ reaction[33].

15. The electronic set-up and the parameters settings of the ^{12}C plastic scintillator detector counting system.

16. The discriminator voltage counting curves for the ^{12}C plastic scintillator detector counting system

17. Sensitivity versus average energy of neutron source for moderated indium foil activation detector. Relative sensitivity of Stephens' results[35] are used and are normalized to SLAC's ^{252}Cf data.

18. Neutron dose equivalent sensitivity of the ^{6}LiF (which has a ^{137}Cs gamma sensitivity of 1 V rad^{-1}) in units of V Sv^{-1}.

19. Neutron fluence sensitivity of the ^{6}LiF (which has a ^{137}Cs gamma sensitivity of 1 V rad^{-1}), in units of V cm^{2}.

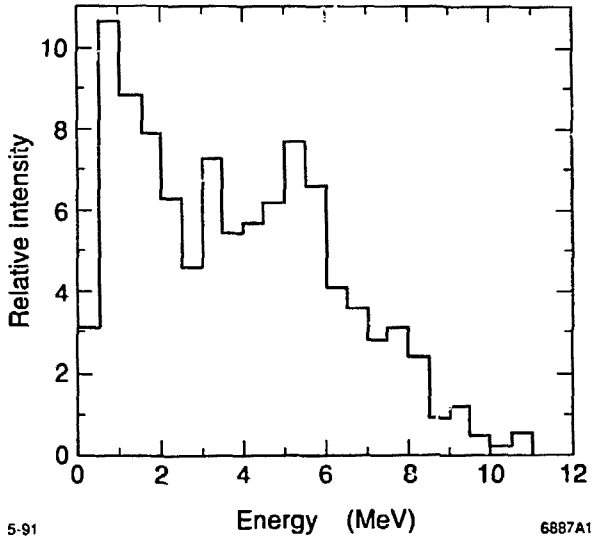

Fig. 1

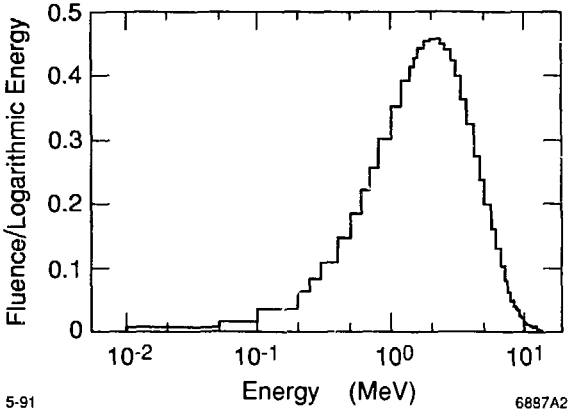
Fluence/Logarithmic Energy
0.5
0.4
0.3
0.2
0.1
0
10^{-2}
10^{-1}
10^{0}
10^{1}
Energy (MeV)
5-91
6887A2

Fig. 2

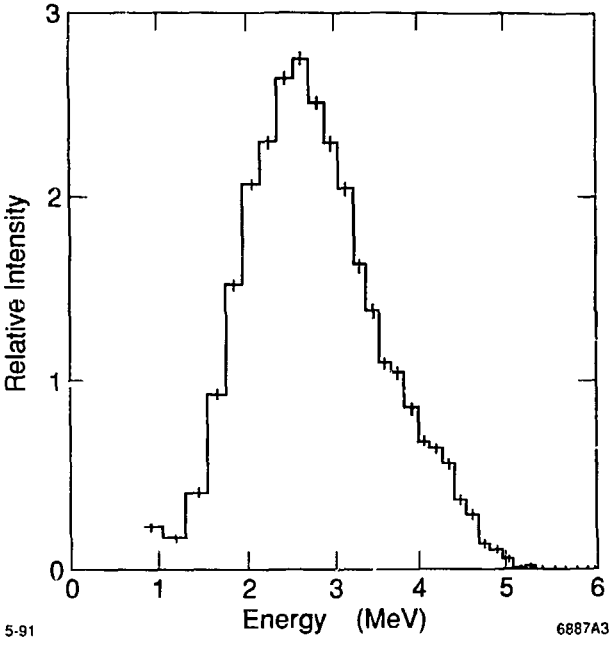
Relative Intensity
3
2
1
0
0
1
2
3
4
5
6
Energy (MeV)
5-91
6887A3

Fig. 3

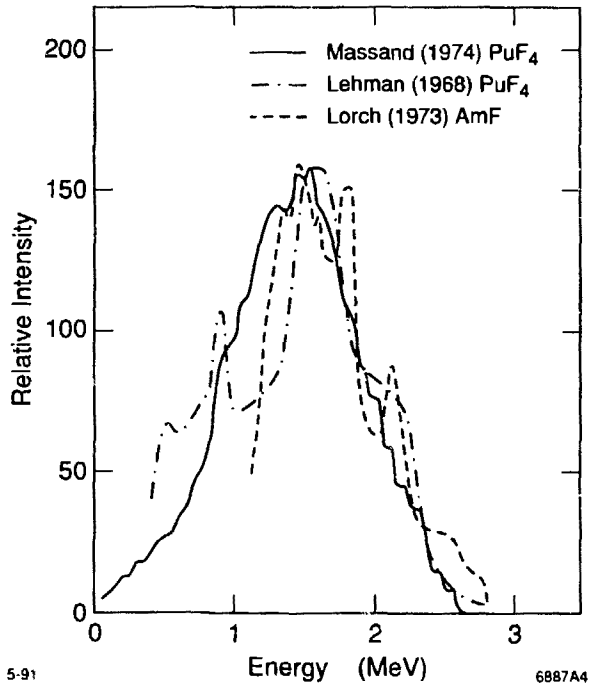
Massand (1974) PuF_4
Lehman (1968) PuF_4
Lorch (1973) AmF
Relative Intensity
200
150
100
50
0
0
1
2
3
Energy (MeV)
5-91
6887A4

Fig. 4

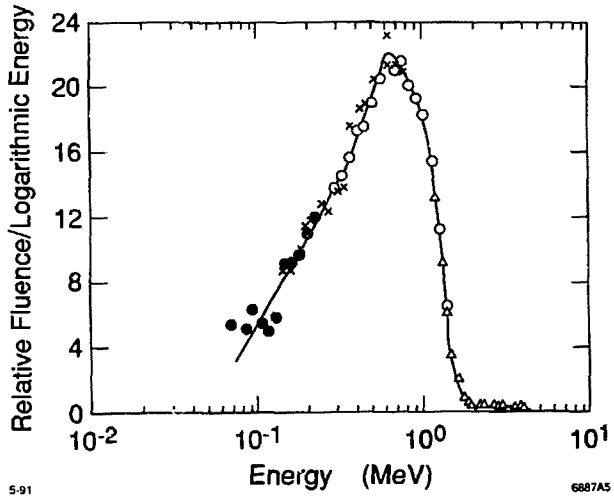
Relative Fluence/Logarithmic Energy
24
20
16
12
8
4
0
10^{-2}
10^{-1}
10^{0}
10^{1}
Energy (MeV)
5-91
6887A5

Fig 5

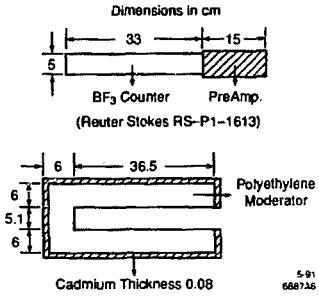
Dimensions in cm
33
15
5
BF3 Counter
PreAmp.
(Reuter Stokes RS-P1-1613)
6
36.5
Polyethylene
Moderator
6
5.1
6
Cadmium Thickness 0.08
5-91
6887A6

Fig. 6

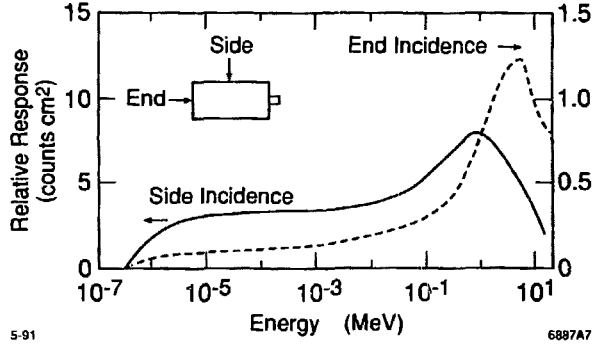
Relative Response
(counts cm2)
15
10
5
0
1.5
1.0
0.5
0
Side
End
End Incidence
Side Incidence
10-7
10-5
10-3
10-1
101
Energy (MeV)
5-91
6887A7

Fig. 7

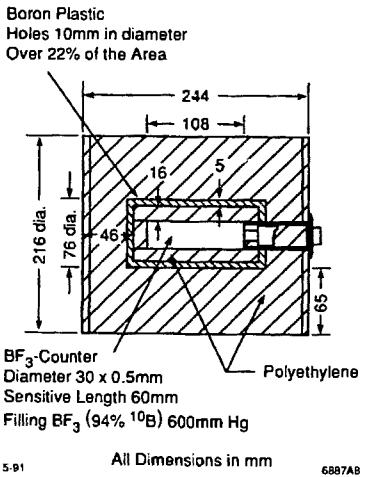
Boron Plastic
Holes 10mm in diameter
Over 22% of the Area
244
108
16
5
216 dia.
76 dia.
46
65
BF3-Counter
Diameter 30 x 0.5mm
Sensitive Length 60mm
Filling BF3 (94% 10B) 600mm Hg
Polyethylene
All Dimensions in mm
5-91
6887A8

Fig. 8

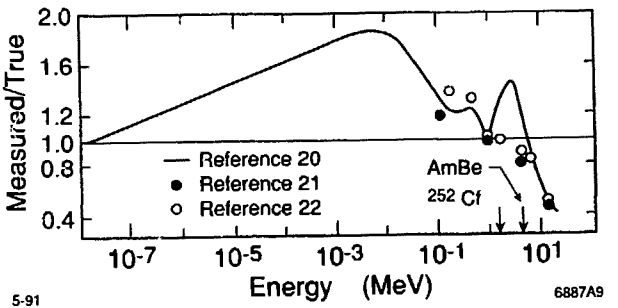
Measured/True
2.0
1.6
1.2
1.0
0.8
0.4
Reference 20
Reference 21
Reference 22
AmBe
252 Cf
10-7
10-5
10-3
10-1
101
Energy (MeV)
5-91
6887A9

Fig. 9

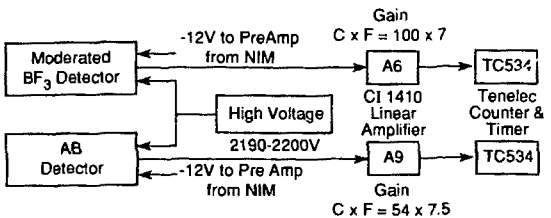
Gain
C x F = 100 x 7
-12V to PreAmp
from NIM
Moderated
BF3 Detector
A6
TC534
CI 1410
Linear
Amplifier
Tenelec
Counter &
Timer
High Voltage
2190-2200V
AB
Detector
A9
TC534
-12V to Pre Amp
from NIM
Gain
C x F = 54 x 7.5
Settings of Amplifiers: 1st Differentiation = 2, 2nd Differentiation = Off
Intergration = Off, Imput Mode = Neg. & Term.
Ouput = Pos.
5-91
6887A10

Fig. 10

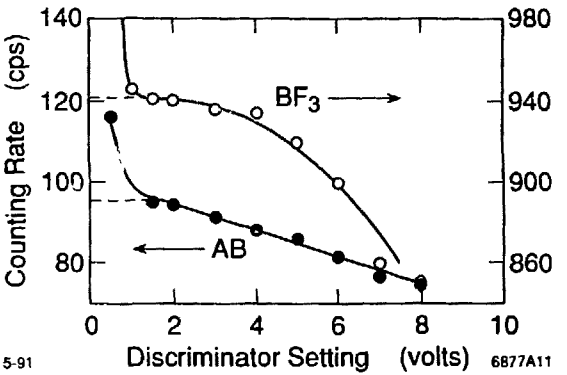
140
120
100
80
980
940
900
860
Counting Rate (cps)
BF3
AB
0
2
4
6
8
10
Discriminator Setting (volts)
5-91
6877A11

Fig. 11

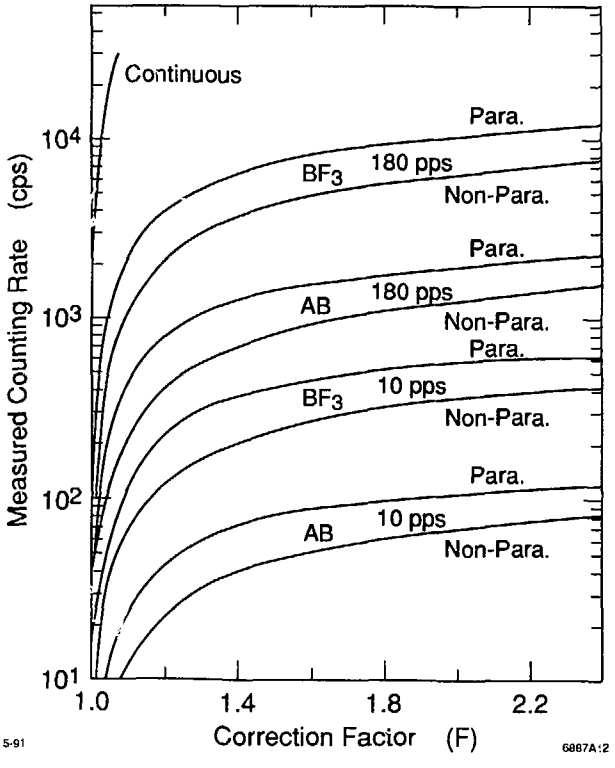
Continuous
Para.
BF3 180 pps
Non-Para.
Para.
AB 180 pps
Non-Para.
Para.
BF3 10 pps
Non-Para.
Para.
AB 10 pps
Non-Para.
Measured Counting Rate (cps)
10^4
10^3
10^2
10^1
1.0
1.4
1.8
2.2
Correction Factor (F)
5-91
6887A:2

Fig. 12

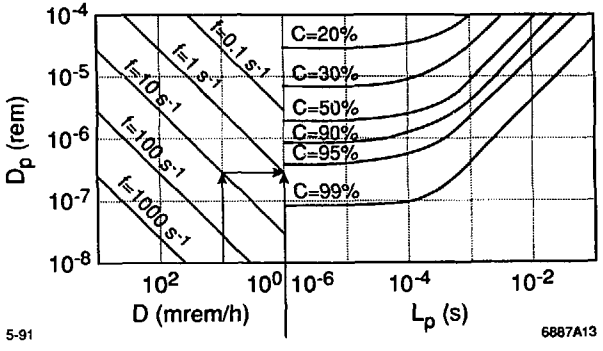
f=0.1 s-1
f=1 s-1
f=10 s-1
f=100 s-1
f=1000 s-1
C=20%
C=30%
C=50%
C=90%
C=95%
C=99%
Dp (rem)
10^-4
10^-5
10^-6
10^-7
10^-8
10^2
10^0
10^-6
10^-4
10^-2
D (mrem/h)
Lp (s)
5-91
6887A13

Fig. 13

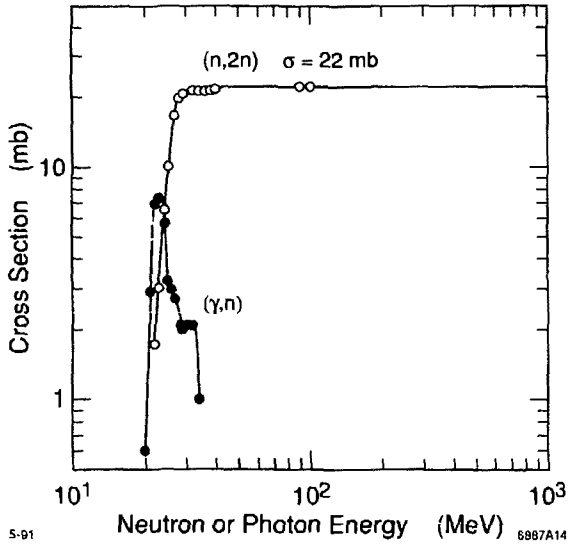
(n,2n) σ = 22 mb
(γ,n)
Cross Section (mb)
10
1
10^1
10^2
10^3
Neutron or Photon Energy (MeV)
5-91
6887A14

Fig. 14

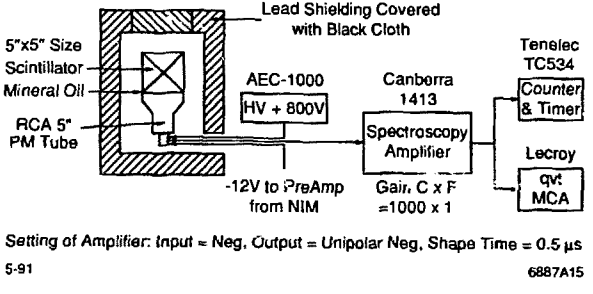
Lead Shielding Covered with Black Cloth
5"x5" Size Scintillator
Mineral Oil
RCA 5" PM Tube
AEC-1000
HV + 800V
-12V to PreAmp from NIM
Canberra 1413
Spectroscopy Amplifier
Gain, C x F =1000 x 1
Tenelec TC534
Counter & Timer
Lecroy
qvt MCA
Setting of Amplifier: Input = Neg, Output = Unipolar Neg, Shape Time = 0.5 μs
5-91
6887A15

Fig. 15

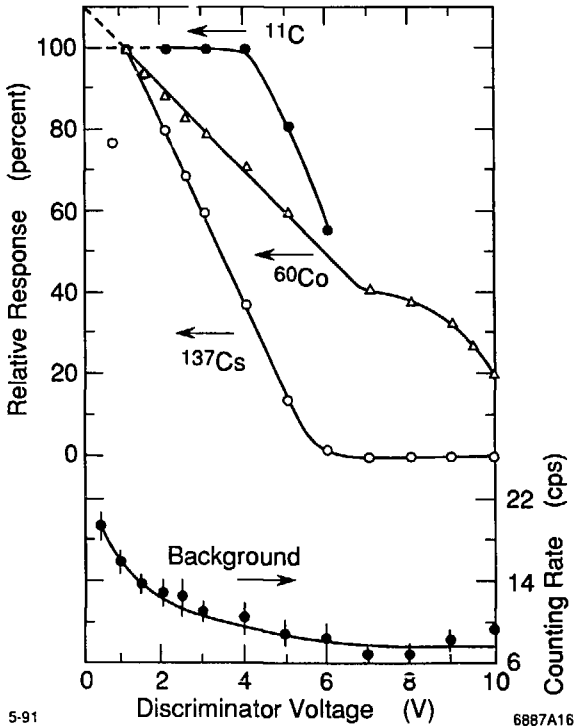
11C
60Co
137Cs
Background
Relative Response (percent)
Counting Rate (cps)
Discriminator Voltage (V)
100
80
60
40
20
0
22
14
6
0
2
4
6
8
10
5-91
6887A16

Fig. 16

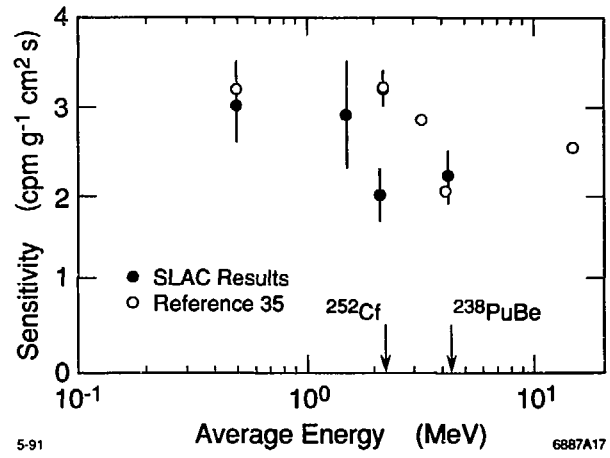
Sensitivity (cpm g-1 cm2 s)
SLAC Results
Reference 35
252Cf
238PuBe
Average Energy (MeV)
4
3
2
1
0
10-1
100
101
5-91
6887A17

Fig. 17

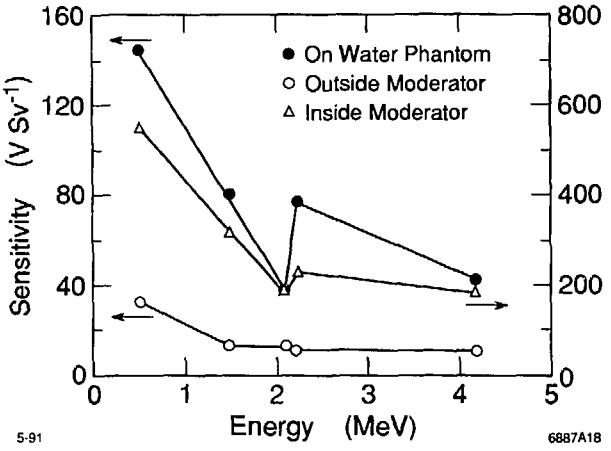
160
120
80
40
0
800
600
400
200
0
Sensitivity (V Sv-1)
On Water Phantom
Outside Moderator
Inside Moderator
0
1
2
3
4
5
Energy (MeV)
5-91
6887A18

Fig. 18

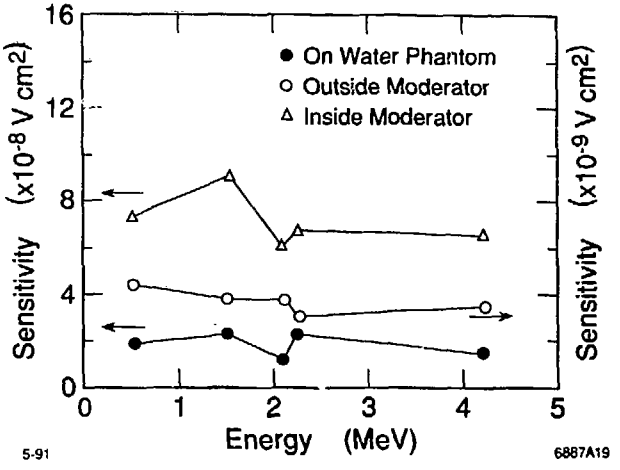
16
12
8
4
0
Sensitivity (x10-8 V cm2)
Sensitivity (x10-9 V cm2)
On Water Phantom
Outside Moderator
Inside Moderator
0
1
2
3
4
5
Energy (MeV)
5-91
6887A19

Fig. 19